Outdoor Experimental Laboratory for Long-Term Estimation of Photovoltaic-Plant Performance

Outdoor Experimental Laboratory for Long-Term Estimation of Photovoltaic-Plant Performance

Alessio Carullo, Alberto Vallan

***Abstract*—This paper describes an outdoor experimental laboratory that has been developed to estimate the performance of photovoltaic plants in operating conditions. The laboratory includes ten different plants and a data acquisition system that has been specifically conceived to monitor the actual behavior of the plants. Main goals of this laboratory are the comparison among the performance indexes of different photovoltaic technologies and the long-term drift estimation of the specifications of the plant components. In this paper, the first results that refer to a time interval of nine months are reported, which allow a comparison among the monitored photovoltaic plants to be performed. A description of the data-acquisition system is also provided by focusing attention towards its metrological management, which allows traceable results to be obtained that are qualified in terms of measurement uncertainty.**

***Index Terms*—Photovoltaic power systems, data acquisition, electric variables measurement, calibration, uncertainty.**

I. Introduction

The interest towards renewable energy, such as solar radiation, wind and tides, has been huge increasing in the last years because of a growing attention with respect to the problems related to the environmental pollution. The employment of such energy sources allows the use of fossil fuels to be drastically reduced, thus reducing the emission of greenhouse gases in the atmosphere: every gigawatthour (GWh) of energy produced thanks to renewable sources prevents up to 10^6 kg of CO_2 emissions. One of the most interesting renewable source is the solar radiation, which allows thermal and electrical energy to be obtained. The latter, which is obtained by means of PhotoVoltaic (PV) cells, is more useful, since it can be used at the production site as well as at great distances thanks to the possibility to integrate a PV plant into the mains. For this reason, in the last decade PV modules based on several technologies have been developed, which are characterized by different cost and performance. Nameplate specifications are usually available for these PV modules that refer to the Standard Test Conditions (STC: solar irradiance 1 kW/m^2, temperature 25 °C, air mass 1.5), but very poor data is available that refers to the long-term drift of the module specifications: this is mainly important for the module efficiency, which is employed to estimate the producibility of a PV plant and, consequently, the pay-back time of the initial investment. A drift of the module efficiency could be taken into account in order to obtain a more realistic estimation.

Authors are with the Dipartimento di Elettronica, Politecnico di Torino, corso Duca degli Abruzzi, 24 - 10129 Torino (Italy); phone: +39 011 0904202, fax: +39 011 0904216, e–mail: alessio.carullo@polito.it

With the aim to overcome this lack of information, authors have developed an outdoor experimental laboratory that is conceived to monitor the actual behavior of different PV plants. The main improvements with respect to similar projects [1]-[9] are the traceability assurance of the obtained results and the qualification of such results in terms of measurement uncertainty. With these goals in mind, the system design has been oriented towards a sustainable metrological management, which is based on a remotely exercised calibration procedure.

In the next sections, a description of the whole system is provided and experimental results that refer to a time interval of nine months are reported. The description of the remote calibration procedure can be found in [10].

II. Outdoor experimental-laboratory architecture

The developed outdoor experimental laboratory, hereafter indicated as PV-LAB (PhotoVoltaic LABoratory), is located in a small-size town of Province of Cuneo (Piemonte - Italy) at a latitude of about 45 °N. It includes ten PV plants based on different technologies and a data acquisition system, which has been designed to estimate the performance of the plants and of their components [11].

The main characteristics of the ten PV plants, which are integrated into the three-phase mains, are resumed in Table I. Five of these plants employ PV modules mounted in a fixed position with a tilt angle β of 35 ° and an azimuth angle γ of about 0 °, while four plants employ PV modules mounted on 2-axis tracking systems. The last plant employs cylindrical modules that are mounted on the horizontal plane ($\beta = 0$ °). The investigated PV technologies are: mono-crystalline silicon, poly-crystalline silicon, string ribbon silicon, Copper Indium Gallium Selenide (CIGS) thin film, cadmium telluride (CdTe) thin film, and High Concentration technology (HCPV).

The ten PV plants are installed in the same site, which is an almost level ground with an area of about 1400 m^2 (48 m·30 m). The data-acquisition system, which is placed in the same site, is 50 m far from the furthest plant. A block scheme of the data-acquisition system the authors have arranged is shown in Figure 1, where the measuring chains of electrical and environmental quantities are highlighted that refer to a single PV plant. The multiplier placed close to each quantity indicates the number of chains included in the system in order to monitor all of the ten PV plants. The measured quantities are:

TABLE I

MAIN CHARACTERISTICS OF THE MONITORED PHOTOVOLTAIC PLANTS

N	PV Technology	Installation	PV module area A_{PV} (m^2)	Total area A (m^2)	PV module efficiency (%)	Array maximum power P_{max} (kW)	PCU efficiency (%)
1	Mono-crystalline silicon	Fixed ($\beta = 35$ °)	11.2	9.2	18.1	2.02	93
2	Poly-crystalline silicon	Fixed ($\beta = 35$ °)	13.8	11.3	13.4	1.85	95
3	String ribbon silicon	Fixed ($\beta = 35$ °)	17.9	14.7	12.7	2.28	93
4	CIGS thin film	Fixed ($\beta = 35$ °)	17.5	14.3	9.6	1.68	95
5	CdTe thin film	Fixed ($\beta = 35$ °)	17.3	14.2	10.1	1.74	95
6	CIGS thin film (cylindrical modules)	Fixed ($\beta = 0$ °)	17.7	17.7	9.7	1.72	92
7	CIGS thin film	Tracking xy	17.5	68.4	9.6	1.68	95
8	CdTe thin film	Tracking xy	17.3	67.5	10.1	1.74	95
9	Mono-crystalline silicon	Tracking xy	11.2	46.3	18.1	2.02	93
10	HCPV	Tracking xy	11.0	45.5	22.0	1.60	92

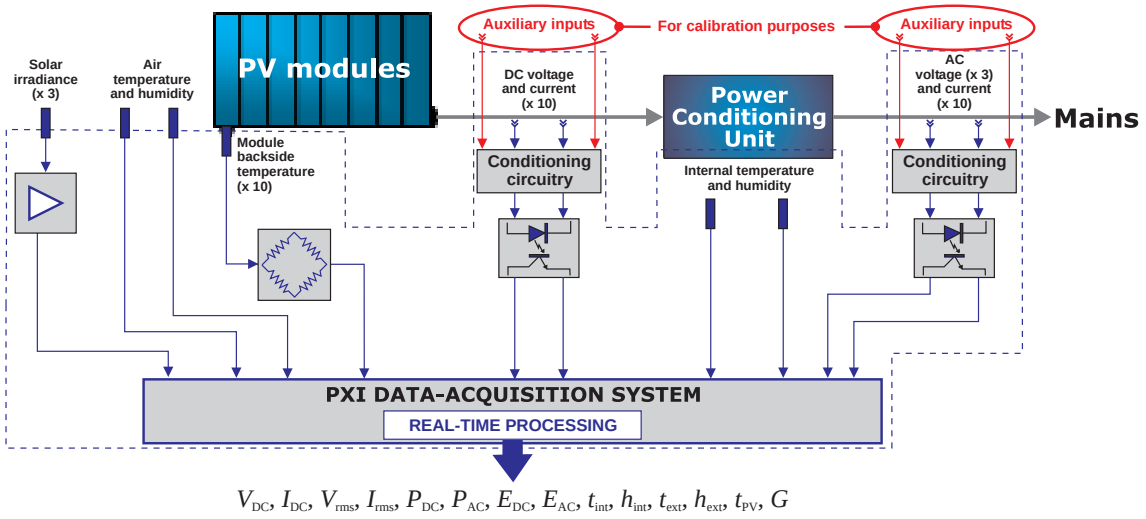

Fig. 1. Block scheme of the data acquisition system.

- DC voltages (10 channels) and currents (10 channels) upstream each Power Conditioning Unit (PCU);
- AC voltages (3 channels since the plants are integrated into a three-phase mains) and current (10 channels) downstream each PCU;
- solar irradiance (3 channels) on the horizontal plane ($\beta = 0$ °) and on the planes of fixed modules ($\beta = 35$ °) and tracking systems;
- module backside temperature (10 channels);
- external temperature and relative humidity (2 channels);
- temperature and relative humidity (2 channels) internal to the site where the PCUs and the data-acquisition system are installed.

AC and DC voltages, whose expected values are 230 V_{rms} and $(100 \div 450)$ V respectively, are conditioned through specifically designed circuits. The voltage to be measured is attenuated by a nominal factor of 70 by means of a resistive divider, then it is sent to a differential amplifier (Burr-Brown INA148), whose single-ended output is connected to a high voltage isolation amplifier (Burr-Brown ISO122). This last component galvanically isolates the plant from the acquisition system, thus avoiding grounding problems that could introduce high noise components into the measuring chain. The isolation also allows equipment and operators to be protected against over-voltages.

AC and DC currents, which are expected in the ranges $(0.5 \div 8)$ A_{rms} and $(0.5 \div 6)$ A respectively, are attenuated by a nominal factor of 1000 by means of thru-hole Hall effect sensors (Honeywell CSNP661), which also ensure the galvanic isolation. The outputs of the current sensors are converted into voltage signals through low temperature-coefficient (25 ppm/°C) film resistors and then amplified by a nominal gain of 4 through an active low-pass filter.

Voltage and current conditioning circuits have been calibrated before starting the monitoring of the PV plants (see section A), thus compensating for initial gain and offset errors. Then, the expected uncertainty has been estimated by taking into account the contributions related to non linearity, time and thermal drift and frequency response for the AC quantities. Since time-drift specifications are not available for all the employed components, authors have estimated this contribution from similar devices, obtain-

ing a standard uncertainty of 0.3% over a time interval of one year.

The solar irradiance is sensed by means of three broadband pyranometers (Kipp&Zonen CMP11), which are installed on the three planes of interest. The nominal sensitivity of the pyranometers is 10 μV/W/m^2, therefore voltage signals not greater than 10 mV are expected for irradiance values that do not exceed 1000 W/m^2. Since the furthest pyranometer is 15 m far from the acquisition system, low noise circuits based on the instrumentation amplifier INA116 have been connected to the pyranometer outputs. The gain of these amplifiers has been set to 200 and their output range is of 3 V, thus allowing theoretical irradiance values up to 1500 W/m^2 to be sensed. The developed circuits also embed an auto-compensation function of the voltage offset and is characterized by a very low bias current (100 fA maximum), thus making negligible the voltage drop across the pyranometer output-resistance, whose value could reach 100 Ω. The relative standard uncertainty of the measured solar irradiance is of 1.2%, which is mainly due to the calibration uncertainty of the pyranometers and to their instrumental daily uncertainty.

The module temperatures are sensed by means of class-A Resistive Thermal Detectors (RTD) Pt1000, which are attached to the backside of a module of each PV plant. A 3-wire configuration is employed to connect each RTD to a bridge circuit, which converts the resistance changes into voltage signals ensuring an absolute standard uncertainty of 0.6 °C in the measurement range from −10 °C to 80 °C. Commercial thermo-hygrometer probes (Rotronic HC2-S) are used to measure external and internal temperatures and humidities. Such probes provide voltage output-signals and ensure standard uncertainties of 0.1 °C and 1 %RH in the measurement ranges $(-40 \div 60)$ °C and $(5 \div 95)$ %RH respectively.

The voltage signals the described measuring chains provide are sent to a PCI eXtension for Instrumentation (PXI) chassis, which embeds three DAQ boards. AC electrical quantities (10 currents + 3 voltages) are acquired by means of a DAQ board NI PXI 6254 (resolution: 16 bit; maximum sampling frequency: 1 MSa/s scanning; 32 single-ended analog inputs) with a sampling rate of 20 kSa/s. DC electrical quantities (10 currents + 10 voltages) are instead acquired by a DAQ board NI PXI 6224 (resolution: 16 bit; maximum sampling frequency: 250 kSa/s scanning; 32 single-ended analog inputs) with a sampling rate of 10 kSa/s. Another DAQ Board NI PXI 6224 acquires the environmental quantities (10 backside module temperatures + 3 solar irradiance + 2 temperatures + 2 relative humidities) and the supply voltage of the bridge circuits that convert RTD changes into voltage changes with a sampling rate of 1 kSa/s.

A custom software, which has been developed in the LabVIEW$^{\text{TM}}$ environment, manages the acquisition system according to the flow chart of Figure 2, where continuous lines refer to the program flow, while dashed lines indicate the data flow. When the Virtual Instrument (VI) is started, the calibration constants of the different measuring chains are loaded and a file is created (if it does not exist), whose name is the current date. Then a timer is started with a period of 2 s, which is the nominal acquisition interval. As soon as the timer period elapses, the scanning of the three DAQ boards is simultaneously started and samples from each board are acquired by multiplexing the active channels. For the AC quantities, 4000 samples are acquired, which nominally corresponds to ten periods of the mains, i.e. 200 ms. During the same time interval, 2000 samples of the DC quantities and 200 samples of the environmental quantities are acquired. A real-time data-processing is then implemented by taking into account the calibration constants of the different chains and provides the quantities of interest:

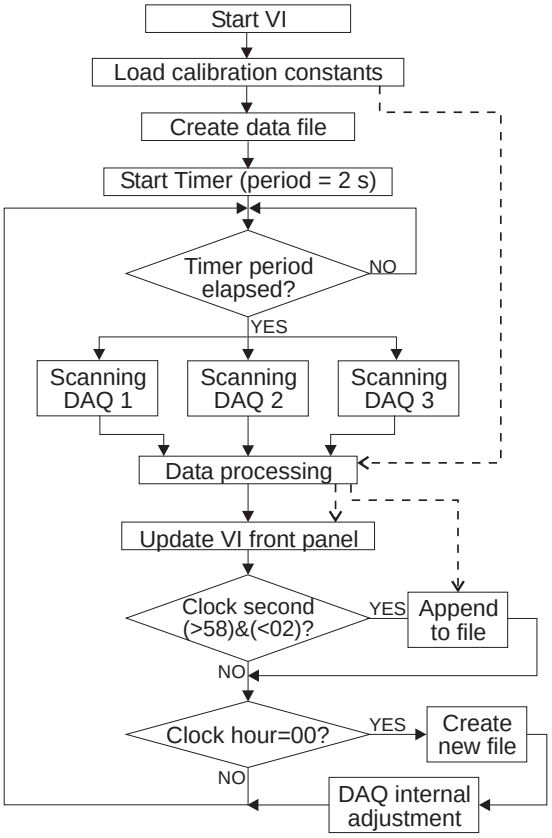

Fig. 2. Flow-chart representation of the acquisition process.

- DC voltages and currents (V_{DC} and I_{DC});
- root mean square value of AC voltages and currents (V_{rms} and I_{rms});
- instantaneous power upstream (P_{DC}) and downstream (P_{AC}) the PCUs;
- DC and AC produced energy (E_{DC} and E_{AC});
- internal and external temperatures and humidities (t_{int}, h_{int}, t_{ext} and h_{ext});
- module backside temperatures (t_{PV});
- solar irradiance G on horizontal plane, tilted plane and on the plane of the 2-axis tracking system.

Samples of the AC quantities are weighted by means of a Hanning window in order to minimize the effects of the non-coherent sampling. DC and environmental quantities

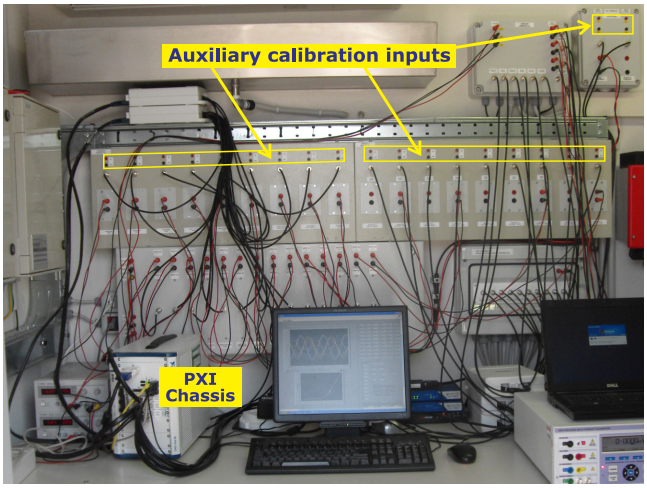

Fig. 3. A photograph of the data-acquisition system.

are estimated by averaging the acquired samples, thus minimizing noise effects. The estimated quantities are used to update the VI front panel at each acquisition step, while the data file is updated with a sample rate of 1 min.

As highlighted in the flow chart, at the midnight of each day, an internal calibration of the three DAQ boards is performed, thus compensating for offset and gain drift. In such a way, the uncertainty related to the DAQ boards is maintained negligible with respect to the other contributions.

The quantities stored into the daily files are off-line processed in order to obtain the performance indexes described in the section B.

III. Experimental results

A. Metrological management of the acquisition system

The outdoor experimental laboratory, which has been running since April 2010, is managed in a controlled way from a metrological point of view, in order to ensure measurement traceability.

Initially, the calibration constants of DC and AC electrical measuring chains have been estimated by stimulating the auxiliary inputs of the data-acquisition system (see Figure 1 and the picture in Figure 3) by means of a multifunction calibrator. For the measuring chains of the environmental quantities, the manufacturer nameplate calibration constants have been used.

Some days after the calibration, a verification of the whole acquisition system has been carried out. The electrical measuring chains have been verified employing reference values provided by the traveling standard described in [10]. Both DC and AC measurement functions have been verified for the quantities voltage, current and active power. The environmental measurement chains have been verified by comparison with respect to the standard sensors embedded into the same traveling standard. The obtained deviations among reference values and indications of the data-acquisition system have not exceeded the Maximum Admitted Errors (MAE), which have been fixed to twice the expected standard uncertainties. The results obtained for the electrical quantities that refer to this first verification are summarized in the Table II under the column with header 2010 (verification date: March 26^{th} 2010), which shows the maximum deviations that have been obtained among the different measuring chains. The table also reports, under the column 2011, the same results that refer to the verification performed after more than one year (verification date: May 13^{rd} 2011) before performing any adjustment operation. It should be noted that, in this case, the maximum deviation of some chains has exceeded the MAE. Possible reasons of this not-conform behavior could be an underestimation of the time-drift contribution or the time elapsed from the first calibration, which is of about 14 months while the expected standard uncertainties have been estimated for a period of 12 months. This not conform behavior will be further analyzed during the next verification. As a consequence of these results, the uncertainty of the not-conform chains have been increased according to the obtained deviations before using it in the uncertainty estimation of the PV performance indexes. It should be also noted that the confidence interval corresponding to the MAE has been obtained using a coverage factor equal to 2, which corresponds to a confidence level of about 95 % if a normal distribution is assumed for the measured quantities. In this situation, the use of a coverage factor equal to 3, which corresponds to a confidence level of about 99 %, brings to a conform behavior.

Eventually, an adjustment procedure has been performed in order to compensate for the measuring-chain drifts and, after the calibration constants have been updated, the verification of the system has been repeated, which has provided results conform to the MAE.

B. Performance indexes of the monitored PV plants

The investigated performance indexes and the corresponding standard uncertainties are summarized in Table III, where:

- $\overline{P_{\mathrm{AC}}}$ is the hourly average of the AC power;
- P_{max} is the array maximum power (see Table I);
- A is the horizontal area that each PV array takes up (see Table I);
- A_{PV} is the area of the PV modules (see Table I);
- E_{AC} (E_{DC}) is the AC (DC) energy downstream the PCU (upstream the PCU) produced over the time interval T_{G};
- $\overline{G}$ is the average of the solar irradiance over the time interval T_G;
- $\overline{P_{DC}}$ is the average of the DC power over the time interval T_G.

The parameter T_{G} represents the time interval during which all the ten PV plants are simultaneously irradiated; it is a-priori estimated according to the plant topology and the period of the year.

An example of results that refers to the performance index $\overline{\eta_{PV}}$ is shown in Figure 4, where a time period of ten days is considered. In the figure, the line thickness

TABLE II
SUMMARY OF THE VERIFICATION RESULTS.

Verified quantity	Verification range	MAE	2010 (max deviation)	2011 (max deviation)
DC voltage	(100 ÷ 470) V	0.6 %	-0.3 %	0.8 %
DC current	(1 ÷ 7) A	0.6 %	0.2 %	0.7 %
AC voltage	230 V @ 50 Hz	0.6 %	-0.1 %	-0.4 %
AC current	(1 ÷ 10) A @ 50 Hz	0.6 %	0.2 %	0.6 %
DC power	(0.1 ÷ 1.5) kW	0.9 %	0.5 %	1.0 %
AC power	(0.1 ÷ 1.8) kW	0.9 %	0.4 %	1.1 %

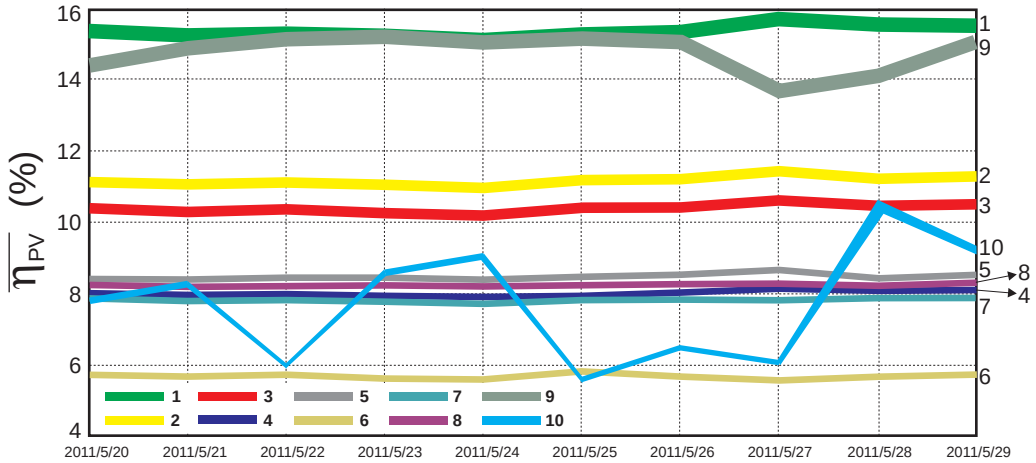

Fig. 4. Example of results for the index $\overline{\eta_{PV}}$ (mean PV efficiency). Line thickness represents the absolute expanded uncertainty.

TABLE III
THE ESTIMATED PERFORMANCE INDEXES

Performance index	Symbol	Definition	Standard uncertainty
Normalized AC power	$P_{\mathrm{AC,norm}}$	$\overline{P_{\mathrm{AC}}}/P_{\mathrm{max}}$	0.45 %
Equivalent hours	h_{AC}	$E_{\mathrm{AC}}/P_{\mathrm{max}}$	0.45 %
Energy area density	$d_{\mathrm{E,A}}$	E_{AC}/A	0.45 %
Mean PV efficiency	$\overline{\eta_{\mathrm{PV}}}$	$\overline{P_{\mathrm{DC}}}/(\overline{G}\cdot A_{\mathrm{PV}})$	1.3 %
Mean PCU efficiency	$\overline{\eta_{\mathrm{PCU}}}$	$E_{\mathrm{AC}}/E_{\mathrm{DC}}$	0.65 %

represents the absolute expanded uncertainty, which have been obtained as twice the standard uncertainty (coverage factor $k = 2$). One should note that the uncertainty of the obtained results, which is mainly due to the calibration uncertainty of the irradiance measuring chain, is suitable for the aim of this work, since it allows the behavior of the different PV plants to be distinguished.

At a first look, Figure 4 shows a good agreement among estimated and nominal PV efficiencies (see Table I) for the plants from 1 to 9. However, as expected the obtained results are all lower than the nominal efficiencies, since the latter refer to the STC that are rarely encountered in real conditions. As well known by literature ([12]-[14]), any variation from the STC affects the PV efficiency. This clearly appears by comparing the couples of plants that employ the same PV modules in fixed and tracking systems (1-9, 4-7, 5-8): since the modules on the tracking systems are perpendicularly irradiated, their backside temperature is greater than the temperature of fixed modules, therefore they exhibit a lower efficiency.

For the plant 10, a comparison of the experimental PV efficiency to the nominal efficiency is meaningless, since modules of this plant embed lens that concentrate the solar radiation on the PV cells. These lens only work in the presence of direct radiation, while the parameter $\overline{\eta_{PV}}$ has been obtained using the global radiation provided by a pyranometer, which includes direct, diffuse and reflected radiation. During the next updating of the data acquisition system, a measuring chain, based on a pyrheliometer, will be added to obtain the direct radiation measurement. The presence of the concentrating lens is also responsible of the large changes that the PV efficiency of the plant 10 shows in the considered period, since it exhibits minimums during cloudy days, while the other plants exhibit a constant behavior.

The frequent out-of-service condition was another poor characteristic of the plant 10, since the lens require a very accurate alignment with respect to the solar radiation, which has not been frequently obtained because of failures at hardware or software components of the tracking system. From a reliability point of view, the availability of this plant was of about 70% in the period from May 2010 to April 2011, while the availability of the other plants was in the range from 91% to 99% in the same period. For this

reason, at the end of April 2011 the tracking system of the plant 10 has been deeply modified: the device that senses the direct radiation and provides the feedback signal for the control of the tracking system has been changed and the software that manages the control strategy has been updated. From then, this plant has properly worked, showing an availability of 100 % in the period from May 2011 to August 2011.

An example of results that refers to the performance index equivalent hours h_{AC} is shown in Figure 5, where the same convention of Figure 4 is employed for the indication of the absolute expanded uncertainty. As expected, the plants that employ PV modules mounted on tracking systems show the best performance, with the exception of the plant 10 for the reasons previously described. On the other hand, these plants have a higher cost for the tracking system itself and for its maintenance. Furthermore, large area are required for their installation (see Table I) thus preventing their use if the available space is the limiting factor.

Among the plants that employ PV module mounted in fixed position, the mono-crystalline silicon technology (1) provides the best producibility performance thanks to its higher efficiency, while poly-crystalline silicon (2), CIGS thin film (4) and CdTe thin film (5) show similar performances that are slightly better than string ribbon silicon (3). This is due to a minor difference among the PV efficiencies of these plants and a lower sensitivity of the thin-film based technologies with respect to the module temperature. Another interesting indication of the Figure 5 is the poor producibility of the plant 6, which uses CIGS thin film cylindrical modules mounted on the horizontal plane. The performance of this technology strongly rely on the solar reflection of the surface that is placed under the modules, but in the monitored plant this surface has not been optimized from a reflection point of view. With the aim to estimate the behavior of this plant in optimum conditions, authors are planning the installation of a commercial white reflecting membrane [15] under the modules.

In order to better distinguish the producibility performance of the different PV plants, the final PV system yield Y_{f} [16] is used, which is defined as:

$$Y_{\mathrm{f}} = \frac{E_{\mathrm{tot}}}{P_{\mathrm{max}}} \tag{1}$$

where E_{tot} is the total energy each plant produces. One should note that the final yield has the same meaning of the parameter equivalent hours already defined, but Y_{f} accounts for the total produced energy, while h_{AC} is limited to the time interval T_{G}.

The final yield Y_{f} that refers to a time interval of nine months is reported in the Table IV, where an expanded uncertainty of 1 % has been considered for the estimation of the uncertainty interval. The period from September 1^{st} 2010 to May 31^{st} 2011 has been considered in order to obtain meaningful indications, since during the first months (from May to August 2010) several failures have occurred at the different PV plants. In the table, the plants are reported in descending order with respect to the parameter Y_{f}; the plant 10 has not been reported for the reason previously described.

TABLE IV

THE FINAL PV SYSTEM YIELD Y_{f} OF THE FIRST NINE PLANTS FROM SEPTEMBER 1^{st} 2010 TO MAY 31^{st} 2011.

N	**PV Technology**	Y_{f} **interval** (kWh/kW)	E_{tot} (kWh)
7	CIGS thin film	1028 ÷ 1048	1744
8	CdTe thin film	982 ÷ 1002	1726
9	Mono-crystalline silicon	971 ÷ 991	1982
1	Mono-crystalline silicon	898 ÷ 916	1832
2	Poly-crystalline silicon	854 ÷ 871	1597
4	CIGS thin film	845 ÷ 862	1435
3	String ribbon silicon	842 ÷ 859	1938
5	CdTe thin film	822 ÷ 838	1444
6	CIGS thin film cylindrical module	489 ÷ 499	850

The obtained results confirm the previous conclusions and also show that, among the plants that employ PV modules mounted on tracking systems, the CIGS thin-film technology (plant 7) provides the greatest producibility. Unfortunately, it is not possible to distinguish the behavior of CdTe thin-film (plant 8) and mono-crystalline silicon technologies (plant 9), since the measurement intervals overlap. For the same reason, it is not possible to distinguish the behavior of the fixed plants that employ poly-crystalline silicon modules (2), CIGS thin film modules (4), and string ribbon silicon modules (3). However, it can be stated that these plants have a better performance with respect to the fixed plant based on CdTe thin film modules (5), but behave worse than the fixed plant that employs mono-crystalline silicon modules (1). Results of Table IV also allow the producibility gain of the PV plants on tracking system with respect to the fixed plants to be estimated. This gain is of 21.5% for the CIGS technology (plant 7 with respect to plant 4) and of 19.5% for the CdTe technology (plant 8 with respect to plant 5). These experimental values are slight lower than the expected ones for the considered nine-month term (27% and 25% respectively), which have been obtained at the PVGIS web site [17]. The main reason of the obtained deviation is the unavailability of the plants 7 and 8, which was of about 4% during the monitored period. For the mono-crystalline silicon technology, the producibility gain of the tracking plant (9) with respect to the fixed plant (1) was only of 8.2%, thus showing a large deviation with respect to the 27% of expected gain. In this case, the unavailability of the plant 9 (about 9% in the considered period) is not sufficient to be considered as the main cause of this large deviation; at the moment, the authors are performing specific investigations to justify this behavior.

Another useful way to express the performance of PV plants consists in using the Performance Ratio PR, which is defined as:

$$PR = \frac{Y_{\mathrm{f}}}{Y_{\mathrm{r}}} = \frac{E_{\mathrm{tot}}/P_{\mathrm{max}}}{H_{\mathrm{tot}}/G_{\mathrm{STC}}} \tag{2}$$

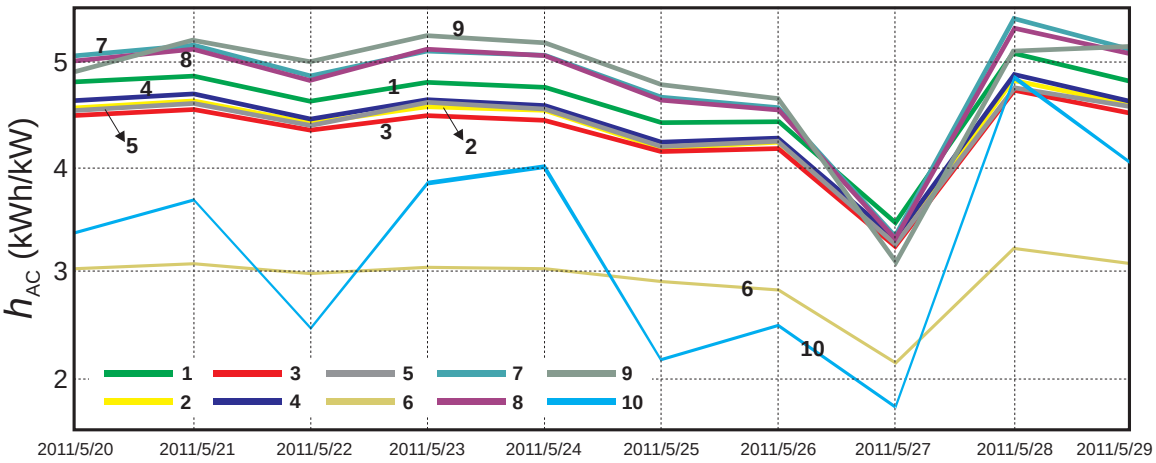

Fig. 5. Example of results for the index h_{AC} (equivalent hours). Line thickness represents the absolute expanded uncertainty.

where the reference yield Y_r is the total irradiation H_{tot} (kWh/m^2) normalized with respect to the STC irradiance G_{STC} (1 kW/m^2). The reference yield hence represents the equivalent number of hours at the reference irradiance. The parameter PR allows all the losses of a PV plant to be highlighted, which are mainly due to PV module temperature effects, PCU inefficiency, wiring losses and module mismatch. Other phenomena the parameter PR takes into account are the effects of the reflection from the module surface, module soiling and system failures.

Figure 6 shows the monthly values of the performance ratio PR for the first nine PV plants in the nine-month period previously considered. In this case, the absolute expanded uncertainty is represented by means of a black box above each bar. It can be observed that PR values in the range from 0.7 to 0.88 have been obtained, with the exception of the plant 6, which shows greater losses due to the bad conditions of the reflecting roof. Figure 6 also allows the seasonal changes of PR to be highlighted: as expected, most of the obtained PR values are greater during the winter, because of the sensitivity of the PV efficiency with respect to the module temperature. This also means that lower PR values are expected during the next summer months.

The producibility of the plant 10 after the modification of the tracking system has improved, but it has never reached the performance of the other plants. As an example, the produced energy in the period June-August 2011 was of 402 kWh against 277 kWh produced during the previous nine months. More information comes from the parameter PR, whose value ranges in the interval $0.32 \div 0.34$ during the last months, while values in the range $0.01 \div 0.11$ was obtained before modifying the tracking system.

The performance ratio PR will be used during next years in order to estimate the long-term performance of the monitored PV plants, which is one of the main goals of the developed outdoor experimental laboratory PV-LAB.

On-line results are available [18] that refer to the performance indexes previously defined.

IV. Conclusion

The described outdoor experimental laboratory is able to estimate the main performance indexes of PV plants with a measurement uncertainty that is suitable to verify manufacturer specifications as well as to compare different PV technologies. The data-acquisition system has been specifically designed in order to be calibrated at a low cost and minimizing the out-of-service interval, since measurement traceability is mandatory in order to obtain meaningful results. The developed data-acquisition system can be also used for diagnostic purposes: an alarm message can be automatically sent to the system manager if the behavior of a plant is not conform with respect to the other plants.

Preliminary results, which refer to a nine-month term, allow interesting evaluation of the different PV technologies to be performed. Results obtained during the next years will be instead employed to estimate the long-term drift of the PV module specifications, thus providing more realistic parameters for the producibility estimation of PV plants based on the investigated technologies.

Acknowledgment

The authors would like to thank engineer Ugo Grimaldi from Ferrero S.p.A. and engineer Stefano Terreno from Energhe S.p.A. for the fruitfully collaboration in the design and development of the outdoor experimental laboratory.

References

[1] X. Xiaoli and Q. Daoe, *Remote monitoring and control of photovoltaic system using wireless sensor network*, IEEE International Conference on Electric Information and Control Engineering (ICEICE), 2011 , April 15-17, pp. 633-638.

[2] D. Thevenard, L. Dignard-Bailey, S. Martel, D. Turcotte, *Performance monitoring of a northern 3.2 kWp grid-connected photovoltaic system*, IEEE Photovoltaic Specialists Conference, 2000, September 15-22, pp. 1711-1714.

[3] E.E. van Dyk, E.L. Meyer, *Long-term monitoring of photovoltaic modules in South Africa*, IEEE Photovoltaic Specialists Conference, 2000, September 15-22, pp. 1525-1528.

[4] M. Benghanem and A. Maafi, *Data Acquisition System for Photovoltaic Systems Performance Monitoring*, IEEE Tr. on IM, Vol. 47(1), February 1998, pp. 30-33.

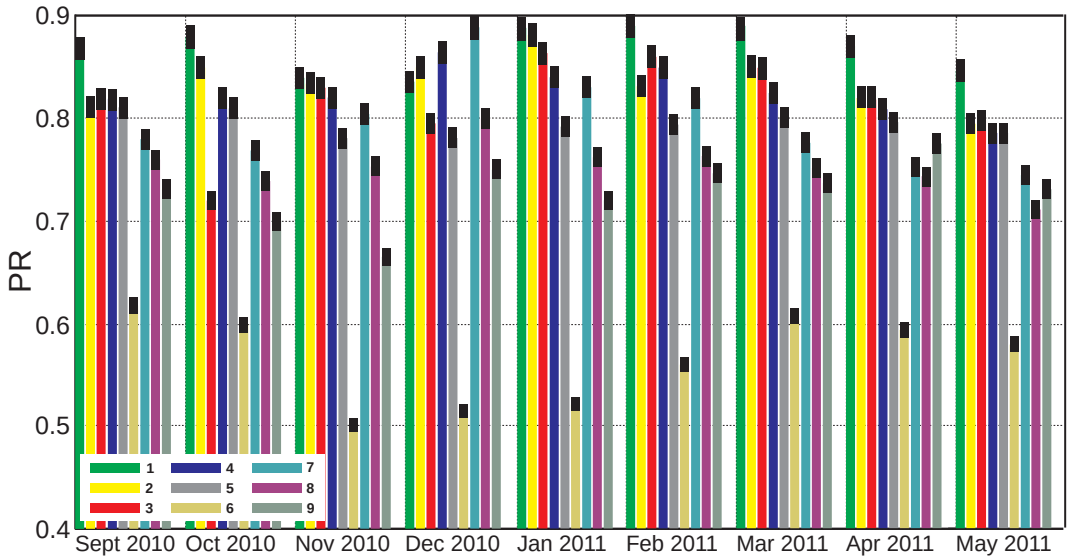

Fig. 6. The performance ratio PR of the first nine plants from September 2010 to May 2011. The black box above each bar represents the absolute expanded uncertainty.

[5] A.J. Carr and T.L. Pryor, *A comparison of the performance of different PV module types in temperate climates*, Solar Energy, Vol. 76(2004), pp. 285-294.
[6] S. Mau and U. Jahn, *Performance Analysis of Grid-Connected PV Systems*, 21st European Photovoltaic Solar Energy Conference and Exhibition, 4-8 September 2006, Dresden, Germany.
[7] E. Dirks, A.M. Gole and T.S. Molinski, *Performance Evaluation of a Building Integrated Photovoltaic Array using an Internet Based Monitoring System*, in Proceeding of IEEE Power Engineering Society General Meeting, pp. 15, 2006.
[8] P. Vorasajan, T.R. Betts, R. Gottschalg and D.G. Infield, *Long-Term Performance of Amorphous Photovoltaic Modules*, 4th World Conference on Photovoltaic Energy Conversion (WCPEC-4), May 7-12, 2006, Waikoloa Hawaii, p. 2129.
[9] G. Makrides et al., *Outdoor Efficiency of Different Photovoltaic Systems Installed in Cyprus and Germany*, 33rd IEEE Photovoltaic Specialists Conference (PVSC '08), May 11-16, 2008, San Diego, California (USA), pp. 1-6.
[10] A. Carullo, S. Corbellini, A. Luoni and A. Neri, *In Situ Calibration of Heterogeneous Acquisition Systems: The Monitoring System of a Photovoltaic Plant*, IEEE Tr. on IM, Vol. 59(5), May 2010, pp. 1098-1103.
[11] A. Carullo, A. Vallan, U. Grimaldi and S. Terreno, *Comparison among photovoltaic technologies: an experimental case study*, I2MTC/2011, May 10-12, 2011, Binjiang, Hangzhou, China, pp. 1299-1304.
[12] E. Skoplaki, A.G. Boudouvis, J.A. Palyvos, *A simple correlation for the operating temperature of photovoltaic modules of arbitrary mounting*, Solar Energy Materials & Solar Cells, Vol. 92, 2008, pp. 1393-1402.
[13] D.L. King, W.E. Boyson, J.A. Kratochvill, *Photovoltaic array performance model*, Sandia Report SAND2004-3535, http://prod.sandia.gov/techlib/access-control.cgi/2004/043535.pdf.
[14] S.R. Williams, T.R. Betts, P. Vorasajan, R. Gottschalg and D.G. Infield, *Actual PV Module Performance Including Spectral Losses in the UK*, 31st IEEE Photovoltaic Specialists Conference (PVSC '05), January 3-7, 2005, Orlando, Florida (USA), pp. 1607-1610.
[15] Renolit Alkorbright membrane at http://www.alkorproof.com, RENOLIT (UK) Cramlington Ltd.
[16] IEC 61724: Photovoltaic system performance monitoring - Guidelines for measurement, data exchange and analysis, 1998.
[17] PhotoVoltaic Geographical Information System, European Commission Joint Research Centre (Ispra, Italy) at http://re.jrc.ec.europa.eu/pvgis/
[18] PhotovoltaicLab at http://www.energhe.com, Energhe S.p.A. - Ferrero group company.

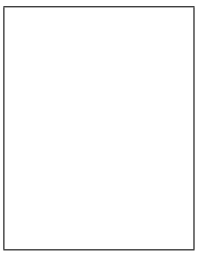

Alessio Carullo was born in Italy in 1966. He received the M.S. degree in Electronic Engineering in 1992 from Politecnico di Torino (Italy) and the Ph.D. degree in Electronic Instrumentation in 1997 from the Università di Brescia (Italy). He is currently with the Politecnico di Torino, Dipartimento di Elettronica, as an Associate Professor of electronic measurements. He works in the development and characterization of intelligent instrumentation and in the validation of automatic calibration systems.

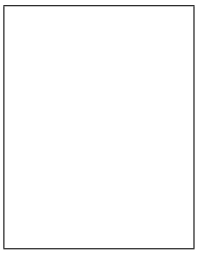

Alberto Vallan received the M.S. degree in Electronic Engineering from Politecnico di Torino (Italy) in 1996 and the Ph.D. degree in Electronic Instrumentation from the University of Brescia (Italy) in 2000. He is currently an assistant professor at the Politecnico di Torino, Dipartimento di Elettronica. His main research interests are in the field of sensors and instruments for industrial applications.